

Study on Extrapolation Method for Self-Propulsion Test with Pre-Swirl Device*

Moon-Chan Kim¹, Yong-Jin Shin¹, Won-Joon Lee², Joon-Hyoung Lee¹

Department of Naval Architecture & Ocean Engineering, Pusan National University, Busan, Korea

²Marine Research Institute, Hyundai Heavy Industries, Co., Ltd., Ulsan, Korea

ABSTRACT

An extrapolation method is proposed for the analysis of a self-propulsion test with a pre-swirl device. Owing to concerns of global warming and the establishing of the Energy Efficiency Design Index (EEDI), energy saving devices are now widely used. In particular, the pre-swirl stator and pre-swirl duct are broadly employed. However, the ITTC 1978 method is not adequate for the prediction of ship performance with a pre-swirl device because the counter swirl component is not viscous; rather, it is a potential term. Moreover, the so-called ITTC 1999 method has not been validated for the pre-swirl device. In this paper, an extrapolation method is thus proposed based on CFD computation, which can extract the tangential velocity component from the total velocity. Two kinds of ships and two kinds of pre-swirl devices were selected for the present computation. The proposed formula can be accurately applied for the analysis of the full-scale performance with a pre-swirl device. Further validation via sea trial results is expected in the future.

Keywords

Energy Efficiency Design Index (EEDI), Extrapolation method, CFD, Effective wake, Pre-swirl device

1 Introduction

In response to the growing concern about global warming and the depletion of fossil fuels, the International Maritime Organization (IMO) has presented the Energy Efficiency Design Index (EEDI) for the building of new ships. The index is based on CO₂ emissions during transport of 1 ton of cargo over 1 sea mile. Since 2013, IMO has ensured that EEDI must be reduced from 10% to 30% until 2025 (Barazi et al., 2011).

Accordingly, studies on energy saving devices (ESDs) are being actively conducted to improve hull forms and propulsion systems. Typical ESDs are the pre-swirl stator (PSS), pre-swirl duct (PSD), contra rotating propeller (CRP), propeller boss cap fin (PBCF), among others.

Located in the front of the propeller, PSS improves the propulsion efficiency through the recovery of rotational energy generated during propeller rotation, thereby engendering a counter-swirl flow against the tangential velocity caused by the propeller. The device achieves an

approximate 5% reduction in energy consumption (Lee et al., 1992; Lee et al., 1994; Kim et al., 1993; Yang et al., 2000; 2001; Kang et al., 2004; Kim et al., 2004). PSD is likewise located in the front of the propeller. It consists of two ESDs: the PSS and duct. The device ensures uniformity of the incoming flow to the propeller. Its performance varies according to the ship type and operating condition, and it reduces energy consumption by 3% to 6% (Mewis and Guiard, 2011; Dang, 2012; Shin et al., 2013; Song et al., 2015).

The ITTC 1978 performance prediction method has been applied to the evaluation of conventional self-propulsion test results for full-scale performance. The so-called ITTC 1999 method was proposed for the full-scale evaluation of a model test for the case of a pre-swirl device. This is because the ITTC1978 method is not adequate for wake scaling in counter-swirl cases. The pre-swirl device influences the flow by both a counter-swirl mechanism and axial retardation. Therefore, existing methods are limited in terms of extrapolation.

The recently proposed extrapolation method for the pre-swirl device (Lee et al., 2015) was applied to the performance analysis of the Kriso Container Ship (KCS) and Kriso Very-Large Crude Oil Carrier 2 (KVLCC2) (Kwon et al., 2013; Kang et al., 2016) with a PSS and PSD. The evaluated results were compared with those evaluated by ITTC 1978 and ITTC 1999 in the present study.

2 Motivation

The powering performance prediction method for the conventional ship model test was successfully established by ITTC in 1978. The ITTC 1978 method was applied to single-screw conventional ships. As mentioned above, PSS and PSD have become widely used as an energy saving device. However, the ITTC 1978 method is limited in terms of the extrapolation method for such a pre-swirl device. Furthermore, the physics of the flow mechanism around the propeller section with the recently proposed ITTC 1999 method has not been elucidated.

2.1 Flow characteristics around the pre-swirl device and propeller

The pre-swirl device creates a counter-swirl flow to reduce rotational energy from the propeller. For the prediction of powering performance, the ITTC 1978 method adopts the thrust identity methodology to determine the effective mean wake fraction. As shown in Figure 1, the angle of attack α depends on the oncoming velocity on the propeller plane (V_A) and the rotational velocity ($2\pi nr$) if the induced velocity is neglected. If the rotational velocity (speed of revolution) is maintained to be the same in the POW condition and the condition of the propeller behind the ship, the oncoming velocity is therefore linear to the thrust. If the pre-positioned device, however, creates a swirl flow that is counter to the propeller inflow, as shown in Figure 1, the respective portion is not viscous; rather, it is a potential flow.

Another issue is that the pre-swirl device creates both a counter swirl and axial flow retardation. It is therefore necessary to separately decompose the axial and tangential portion. If the scaling is applied to the total amount of the model wake in this case, the result may be less than the real full-scale value because the tangential portion should not be scaled.

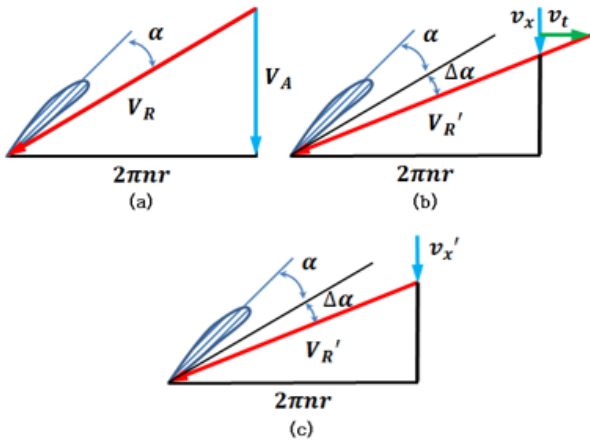


Figure 1 Change of inflow angle at the propeller blade section on account of the induced ESD velocity

2.2 ITTC 1999 method

The combined propulsor, such as the PSS propeller system, can be analyzed with two methods, which are shown in Figure 2. In Method A, the pre-device is deemed a combined propulsor, which means the pre-device and propeller are treated as a whole propulsor. This method is normally used for a contra-rotating propeller. In Method B, the pre-device is regarded as a part of the hull. Therefore, a resistance test is conducted with the pre-device, whereas the POW test is executed with the propeller alone. For Method A, the contra-rotating dynamometer should be used for the POW test. Therefore, Method B is typically on account of this type of restriction.

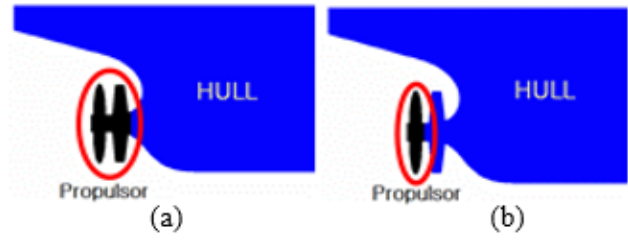


Figure 2 ITTC 1999 method

Table 1 Comparison of results according to prediction method

Method	EHP (PS)	RPM	DHP (PS)	DHP Diff. (%)
W/O Stator	18,058	75.92	25,635	100
ITTC 1978	18,222	74.02	25,250	98.5
Method A	18,058	71.22	24,082	93.9
Method B	18,222	71.34	23,908	93.3

Lee et al. (1992) presented a powering performance comparison for PSS with these two kinds of methods. As shown in Table 1, Methods A and B are almost the same. However, a significant difference exists between them and the ITTC 1978 method. This difference arises from the condition mentioned in Section 2.1. The wake scaling method in the ITTC 1978 method is shown in Equation (1).

$$W_S = (t + 0.04) + (W_M - t - 0.04) \frac{C_{FS} + C_A}{C_{FM}} \quad (1)$$

Where w_S = effective wake with pre-swirl device in full scale; w_M = effective wake without pre-swirl device in model scale; and t = thrust deduction with pre-swirl device in model scale.

The wake scaling approach of the ITTC 1999 method is shown in Equation (2) and is adapted from the Takekuma et al. (1980) method.

$$W_{SS} = (t_{MO} + 0.04) + (W_{MO} - t_{MO} - 0.04) \frac{C_{FS} + C_A}{C_{FM}} + (W_{MS} - W_{MO}) \quad (2)$$

Where w_{SS} = effective wake with pre-swirl device in full scale; w_{MS} = effective wake with pre-swirl device in model scale; w_{MO} = effective wake without pre-swirl device in

model scale; and t_{MO} = thrust deduction without pre-swirl device in model scale.

The last term is separately added because the tangential velocity by the stator should not be scaled. As mentioned above, however, the PSS causes axial velocity retardation for the propeller as well as the count swirl. To compensate the neglected axial flow portion, the thrust deduction without PSS is used instead of the thrust deduction with PSS, as shown in Equation (2). In the present study, the induced velocity by the pre-swirl device is separated into tangential and axial velocity components by CFD analysis.

3 Numerical analysis

3.1 Numerical method and analysis conditions

The CFD solver used for this study was Star CCM+ of CD-adapco, which has been globally used since 2004. The Reynolds averaged Navier–Stokes (RANS) equation was the governing equation used for the three-dimensional unsteady turbulent flow passing over the ship and propeller under the assumption of incompressible and viscous flow. The realizable k- ϵ is used as the turbulent model.

1) Continuity equation

$$\frac{\partial(\rho U)}{\partial x} + \frac{\partial(\rho V)}{\partial y} + \frac{\partial(\rho W)}{\partial z} = 0 \quad (3)$$

2) Momentum equation

$$\frac{\partial(\rho u_i)}{\partial t} + \frac{\partial(\rho u_i u_j)}{\partial x_j} = -\frac{\partial p}{\partial x_i} + \frac{\partial}{\partial x_i} \left[\mu \left(\frac{\partial u_i}{\partial x_j} + \frac{\partial u_j}{\partial x_i} \right) \right] + \frac{\partial}{\partial x_i} (-\rho \overline{u_i u_j}) \quad (4)$$

To resolve the coupling of velocity and pressure, the semi-implicit method for pressure-linked equations (SIMPLE) algorithm was used. The moving reference frame (MRF) method was employed for the rotation model. The computational conditions are shown in Table 2.

The boundary conditions in this study are shown in Figure 3. The velocity inlet condition was applied in the entrance and outer boundary regions, and the pressure outlet condition was applied in the exit region. The trimmer mesh was used for constructing the grid system applied in this study. The CFD calculation was performed with approximately 3,300,000 grids near the ship and 1,700,000 grids in the rotating region.

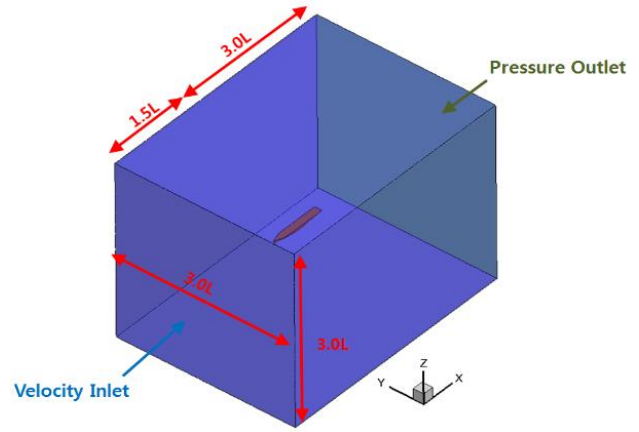


Figure 3 Boundary conditions

Table 2 Analysis condition

	KVLCC2	KCS
Program	Star CCM+ (Ver 9.04)	
Governing Equation	Incompressible RANS Equation	
Discretization	Cell Centered FVM	
Turbulence model	Realizable k- ϵ model	
Wall function	Non-Equilibrium	
Velocity-Pressure Coupling	SIMPLE Algorithm	
Rotation Method	Moving Reference Frame	
Yp	0.0003(Hull), 0.0001(Propeller)	
Cell Number	5,000,000	
Physical Time	45s	

3.2 Validation of CFD calculation

To quantitatively verify the present numerical method, CFD results regarding KCS were compared with the model test results. The tests were performed in PNU's towing tank, and the comparison results are shown in Table 3. A comparison of the nominal wake between CFD and the model test is also shown in Figure 4. A good agreement is apparent between the CFD and EFD results.

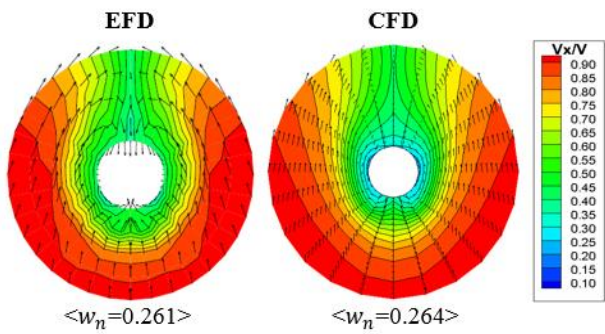


Figure 4 Comparison of nominal wake

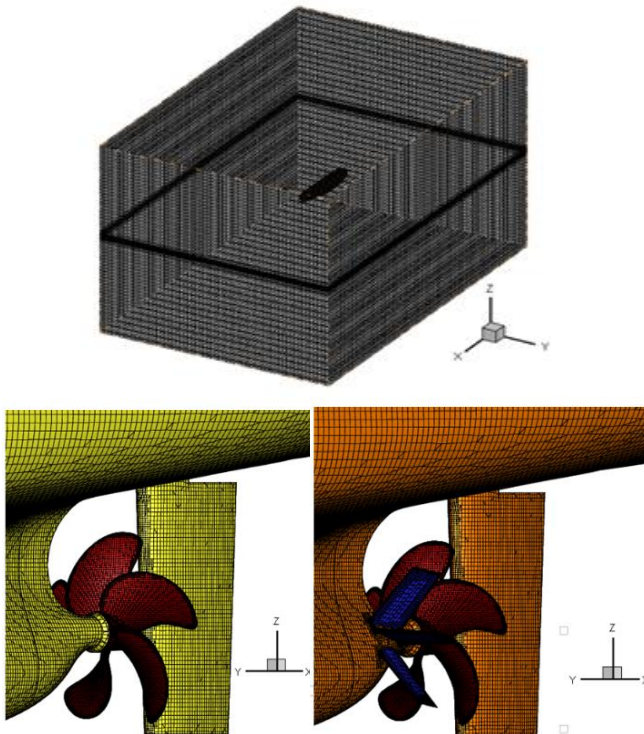


Figure 5 Grid system of KCS

(Top : domain; Left : bare hull; Right : with stator)

Table 3 Comparison between CFD and model test

	$R_{TM}(N)$		
	Bare Hull	With Stator	Diff.(%)
CFD	45.75	46.78	2.25
EFD	45.45	46.30	1.87
Diff.(%)	0.66	1.04	

3.3 Numerical analysis results

To analyze the flow characteristics of the pre-swirl devices, a numerical analysis was conducted by using CFD mentioned above. As shown in Figures 6 and 7, PSD and PSS are equipped in KVLCC2 and KCS, respectively.

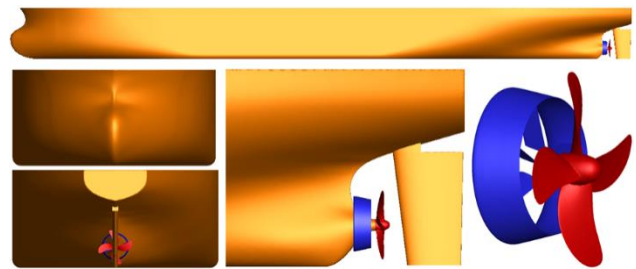


Figure 6 KVLCC2 with PSD



Figure 7 KCS with PSS

3.3.1 Hydrodynamic Force

In a comparison of hydrodynamic force depending on whether a pre-swirl device was installed, the values of drag and thrust with the pre-swirl device were larger than those without the pre-swirl device. The value of the revolution speed with the pre-swirl device was smaller than without the pre-swirl device. The results are shown in Tables 4 and 5.

Table 4 Hydrodynamic forces of KVLCC2

15.5kts	Drag (N)	Thrust (N)	Torque (N-m)	rps
Bare	64.08	42.27	1.12	8.61
PSD	65.36	43.31	1.13	8.45
Diff. (%)	2.00	2.44	0.86	-1.86

Table 5 Hydrodynamic forces of KCS

24.0kts	Drag (N)	Thrust (N)	Torque (N-m)	rps
Bare	52.54	34.11	1.156	10.71
PSS	54.02	35.04	1.123	10.65
Diff. (%)	2.82	2.73	-2.85	-0.56

3.3.2 Wake components

To analyze the effect of the pre-swirl device, we drew components of axial velocity and tangential velocity in the propeller plane. The results are shown in Tables 6 and 7.

Table 6 Wake components of KVLCC2

15.5(kts)	Wake	V_x/V	V_t/V
Propeller Plane	Bare	0.954	0.243
	PSD	0.952	0.203
	Diff.(%)	-0.2	-16.8

Table 7 Wake components of KCS

24.0(kts)	Wake	V_x/V	V_t/V
Propeller Plane	Bare	0.918	0.149
	PSS	0.871	0.062
	Diff.(%)	-5.1	-58.8

4 Analysis of results and new extrapolation formula

The present approach is based on the concept of the thrust being linearly correlated with the angle of attack. This was used in the evaluation of the model mean wake in the ITTC1978 method, as shown in Figure 1. The increased portion of the mean wake by the pre-swirl device can be divided into the portion due to the axial flow retardation and to the counter swirl flow, which make the angle of attack increase in both cases. By using the computed results, the modified formula from the ITTC1999 method is proposed for each kind of vessel. The presently proposed

formula is actually applied to the extrapolation of the model test results.

4.1 Analysis of the angle of attack portion

The angle of attack of flow to the propeller is decided by the combination of the mean axial inflow velocity, rotational inflow velocity, and pitch angle. In the present study, mean volumetric velocity and pitch angle were used for the calculation of the contribution portion of axial and tangential flow by the pre-swirl device. Each case of mean flow and angle of attack portions are shown in Tables 8 and 9.

The portion of the angle of attack by the tangential flow with the PSS is larger than that of axial flow, while the portion by the axial flow with the PSD is larger than that by the tangential flow.

Table 8 Angle of attack portion of KVLCC2

Angle of attack (Degree)	With Pre-Swirl Duct
	Propeller Plane
Bare, $V_{Axial} + V_{Tangential}$	1.536
PSD, $V_{Axial} + V_{Tangential}$	1.644
Portion of V_{Axial} (%)	79
Portion of $V_{Tangential}$ (%)	21

Table 9 Angle of attack portion of KCS

Angle of attack (Degree)	With Pre-Swirl Stator
	Propeller Plane
Bare, $V_{Axial} + V_{Tangential}$	0.420
PSS, $V_{Axial} + V_{Tangential}$	1.555
Portion of V_{Axial} (%)	33
Portion of $V_{Tangential}$ (%)	67

4.2 Proposed formula for extrapolation of full-scale wake

If the tangential and axial velocity component contributing to the angle of attack can be divided as shown in Section 4.1, the new extrapolation formula can be as shown in Equation (5). In this equation, the thrust deduction factor is changed from that without the pre-swirl device in the ITTC 1999 method to that with the pre-swirl device. As shown in Tables 8 and 9, the portions by the tangential and the axial flow are different according to the different vessels and devices. As shown in Table 10, in the present study, the proposed factors of axial and tangential portions are 0.3 and 0.7 in the PSS case and 0.8 and 0.2 in the PSD case, respectively.

$$w_{SS} = (t_{MS} + 0.04) \quad (5)$$

$$+ (w_{MS,Axial} + t_{MS} - 0.04) \frac{C_{FS} + C_A}{C_{FM}} + w_{MS,Tangential}$$

$$w_{MS,Axial} = w_{MO} + (w_{MS} - w_{MO}) \cdot Factor_{Axial} \quad (6)$$

$$w_{MS,Tangential} = (w_{MS} - w_{MO}) \cdot Factor_{Tangential} \quad (7)$$

Where w_{SS} = effective wake with pre-swirl device in full scale; w_{MS} = effective wake with pre-swirl device in model scale; w_{MO} = effective wake without pre-swirl device in model scale; and t_{MS} = thrust deduction with pre-swirl device in model scale.

Table 10 Factors of axial and tangential portion

ESD Type	$Factor_{Axial}$	$Factor_{Tangential}$
PSS	0.3	0.7
PSD	0.8	0.2

4.3 Application to the extrapolation method

The proposed method was applied to the extrapolation method in a comparison with the ITTC 1978 and ITTC 1999 methods. As shown in Table 11, the thrust deduction results with and without PSD were almost the same, which was the case for PSS as well. The evaluated results of full-scale wake are shown in Table 12. The results of PSS with the proposed method are located between ITTC78 and 99. They are closer to the ITTC99 results. The PSD results are also between ITTC78 and 99; however, they are closer to those of ITTC78. The delivered power and speed of revolution were also evaluated by this wake and thrust deduction shown in Tables 13 and 14. The tendency of the delivered power and revolution speed are the same as the full-scale wake fraction.

Table 11 Comparison of thrust deduction

Ship Type		Bare (1978)	ESD (1978)	ESD (1999)	ESD (K&L)
KVLCC2 PSD	t_S	0.234	0.235		
	Diff. (%)	-	+0.43		
KCS PSS	t_S	0.172	0.174		
	Diff. (%)	-	+1.16		

Table 12 Comparison of effective wake

Ship Type		Bare (1978)	ESD (1978)	ESD (1999)	ESD (K&L)
KVLCC2 PSD	w_S	0.342	0.363	0.383	0.367
	Diff. (%)	-	+6.14	+11.99	+7.31
KCS PSS	w_S	0.254	0.282	0.303	0.298
	Diff. (%)	-	+11.02	+19.29	+17.32

Table 13 Comparison of delivered power

Ship Type		Bare (1978)	ESD (1978)	ESD (1999)	ESD (K&L)
KVLCC2 PSD	P_D (PS)	26226	24959	24384	24793
	Diff. (%)	-	-4.83	-7.02	-5.46
KCS PSS	P_D (PS)	43,672	42,857	41,833	42,094
	Diff. (%)	-	-1.87	-4.21	-3.61

Table 14 Comparison of speed of revolution

Ship Type		Bare (1978)	ESD (1978)	ESD (1999)	ESD (K&L)
KVLCC2	RPM	71.73	70.42	69.53	70.23
	PSD Diff. (%)	-	-1.83	-3.07	-2.09
KCS	RPM	106.28	105.19	103.73	104.11
	PSS Diff. (%)	-	-1.03	-2.40	-2.04

5 Discussion and Conclusion

The present study addressed the extrapolation method of the model wake for the case of a pre-swirl device, such as PSS and PSD. The ITTC 1999 method has been used for these kinds of devices because the rotational flow due to the pre-swirl device should not be scaled. The ITTC 1999 method, however, is not physically accurate for that case because the axial retardation due to the pre-swirl device also occurs in the portions that should be scaled. The CFD technique is used for the separation of axial and tangential flows for the case of KCS and KVLCC2 with the PSS and PSD, respectively. The present prediction method was thus proposed. Detailed conclusions are as follows:

1) The pre-swirl device causes axial flow retardation as well as a counter-swirl flow. The portion of the increase of angle of attack by the axial and tangential flow is different in each PSS and PSD; the tangential portion with the PSS is larger than that with the PSD, whereas the axial portion in the PSD is larger.

2) The proposed extrapolation formula for the scaling of the model wake was proposed as shown in Equation (5). The model wake w_M , which is simply the added term of $(w_M - w_s)$ in the ITTC 1999 method, is separated into $w_{MS,Axial}$ and $w_{MS,Tangential}$. According to the pre-swirl device and ship type, the portion (factor) can be decided by the analysis of the flow field disturbed by the pre-swirl device (here, CFD). If the ship astern shape and pre-swirl device are not very different, the proposed factor can be used without further computations if the astern shape and device are not significantly different. The proposed factor is shown in Table 10.

3) The proposed method was applied to the evaluation of the full-scale effective wake, delivered power, and revolution speed for the KVLCC2 with PSD and KCS with PSS in a comparison of the ITTC1978 and ITTC1999 methods. As shown in Table 12, in terms of the portion of the pre-swirl device contribution, the results of each full-scale value with the presented method for PSS are similar to those of the ITTC1999 method results; however, they show a slight shift toward the ITTC1978 method results.

On the other hand, for PSD, their results are rather similar to those of the ITTC1978 method, which likewise showed a slight shift toward those of the ITTC1999 method.

4) The proposed method is expected to be validated by an experiment, such as LDV or PIV. Moreover, the proposed method can be improved by full-scale feedback data.

ACKNOWLEDGEMENTS

This work was supported by a National Research Foundation of Korea (NRF) grant funded by the Ministry of Knowledge Economy (MEST) of the Korean government through GCRC-SOP.

REFERENCES

- Zabi Bazari, Tore Longva, (2011). 'Assessment of INO-mandated energy efficiency measures for international shipping'. Project Final Report, MEPC 63/INF.2, Annex
- ITTC. '1978 ITTC Performance Prediction Method'. ITTC Recommended Procedures and Guidelines, Section 7.5-02-03-01.4, Effective Date. 2014, Revision. 03.
- ITTC (1999). 'Final report of the specialist committee on unconventional propulsors', 22nd International Towing Tank Conference, Seoul Korea and Shanghai, China.
- Kwon, J. I. (2013). 'A study on biased asymmetric pre-swirl stator for container ship'. Master's thesis. Pusan National University.
- Kang, J. G. (2013). 'A study on Performance of Pre-Swirl Stator According to Shape for KCS'. Master's thesis. Pusan National University.
- Lee, W. J. (2015). 'Study on Full-Scale Performance Prediction for Pre-Swirl Device Model Test Results'. Doctor's thesis. Pusan National University
- Kim M.C., Chun H.H., Kang Y.D. (2004). 'Design and Experimental Study on a New Concept of Preswirl Stator as an Efficient Energy-Saving Device for Slow Speed Full Body Ship'. SNAME, pp.111-121
- Lee J.T., Kim M.C., Suh J.C., Kim S.H., Choi J.K. (1992). 'Development of Preswirl Stator-Propeller System for Improvement of Propulsion Efficiency : a Symmetric Stator Propulsion System'. Journal of the Society of Naval Architects of Korea, 41(3), pp.13-21
- Lee J.T., Kim M.C., Van S.H., Kim K.S., Kim H.C., (1994). 'Development of Preswirl Stator-Propeller System for a 300K VLCC'. Journal of the Society of Naval Architects of Korea, 31(1), pp.1-13
- Kang Y.D., Kim M.C., Chun H.H.. (2004). 'A Study on the Asymmetric Preswirl Stator System'. Journal of the Society of Naval Architects of Korea, 44(3), pp.13-21
- Yang J.M., Lee S.J., Kim H.C., Suh J.C., Park Y.M., (2000). 'Effect of pre-swirl stator vane on the

- propeller hull interaction of a full ship'. Proceedings of the Annual Autumn Meeting, SNAK, Ulsan, pp.188-191.
- Yang J.M., Kim K., Park K.H., Kim H.C., Suh J.C., Park Y.M., (2001). 'Effect of pre-swirl stator vane on the propeller hull interaction(2)'. Proceedings of the Annual Autumn Meeting, SNAK, Seoul, pp.216-219.
- Mewis F. and Guiard T., (2011). 'Mewis duct-new developments, solutions and conclusions'. Second International Symposium on Marine Propulsors, Hamburg, Germany..
- Dang J., (2012). 'An exploratory study on the working principle of energy saving devices(ESDs)-PIV,CFD investigations and ESD design guidelines'. Proceedings of the 31st International Conference on Ocean, Offshore and Arctic Engineering, OMAE2012-83053, Rio de Janeiro, Brazil.
- Shin H.J., Lee J.S., Lee K.H., Han M.R, Hur E.B., Shin S.C., (2013). 'Numerical and experimental investigation of conventional and unconventional preswirl duct for VLCC'. International Journal of Naval Architecture and Ocean Engineering, 5(2), pp. 414-430..
- Song H.J., Kim M.C., Lee W.J., Kim J.H., (2015). 'Development of the New Energy Saving Device for the Reduction of Fuel of 176k Bulk Carrier'. Journal of the Society of Naval Architects of Korea, 52(6), pp. 419-427..
- Takekuma K., (1980). 'Evaluation of Various Types of Nozzle Propellers and Reaction Fin as a Device for the Improvement of Propulsive Performance of High Block Coefficient Ship'. SNAME Shipboard Energy Conservation Symposium, pp. 74-84.
- Kim K.S., Kim M.C., Van S.H., Suh J.C., Lee J.T., (1994). 'A Preswirl stator-Propeller system as a Reliable Energy-Saving Device'. Proceedings of Propeller/Shafting`94 Symposium, Virginia Beach, pp. 9-1~9-16..
- Lee J.T. et al, (1992). 'Development of a Preswirl Stator – Propeller System(II)'. KRISO Report, UCK009-1655D.